Available online at www.sciencedirect.com
SCIENCE DIRECT®
International Journal of Heat and Mass Transfer 48 (2005) 1117–1127
International Journal of HEAT and MASS TRANSFER
www.elsevier.com/locate/ijhmt

Solution of transport equations on unstructured meshes with cell-centered colocated variables. Part I: Discretization

A.W. Date *

Mechanical Engineering Department, Indian Institute of Technology, Bombay, Powai, Mumbai 400 076, India

Received 2 April 2004; received in revised form 9 September 2004
Available online 8 December 2004

Abstract

This paper describes discretization of transport equations on unstructured meshes with cell-centered colocated variables. The problem of zig-zag pressure prediction is eliminated by introducing *smoothing pressure correction* derived by Date [A.W. Date, Complete pressure correction algorithm for solution of incompressible Navier–Stokes equations on a non-staggered grid, Numer. Heat Transfer, Part B 29 (1995) 441–458]. The finite-volume discretization is carried out in a structured grid like manner by invoking a special *line-structure* to evaluate convective–diffusive transport across the cell-faces.

Keywords: SIMPLE algorithm; Smoothing pressure correction; Unstructured meshes; Colocated variables; Line-structure

1. Introduction

There is considerable interest in solving transport equations of flow and energy transfer on unstructured meshes because of the suitability of the latter to map complex domains. Unstructured meshes are formed by connecting arbitrary distribution of points (called *vertices*) within a given domain by non-intersecting lines. This results in formation of polygonal elements (or, cells) in 2D domains and polyhedral elements in 3D domains. To carry out finite-volume discretization, it is necessary to define a node along with a control-volume (CV) surrounding that node. Three approaches are possible:

In the *Vertex-Centered* approach, the vertices are taken as nodes and a CV is specially constructed as shown in Fig. 1a for a 2D mesh. In this figure, the CV is formed by joining *centroids* of successive elements surrounding vertex P [7] but, other conventions are also possible [13,12]. Note that the line joining P to its neighbouring vertices will, in general, not be orthogonal to the control-volume faces (shown by dotted lines). Also, node P will not be at the centroid of the CV in general but, the CV will always enclose the node.

The second, called the *Circum-Centred* approach, defines nodes at the circumcentre of each cell (see Fig. 1b). One advantage of this approach is that the cell-face shared by two neighbouring elements will always be orthogonal to the line joining the circumcentres which are treated as nodes. However, a serious disadvantage is that the circumcentre of each cell may, in general, not lie *within* the cell. This is shown by node E in Fig. 1b.

The third, and the most popular approach, defines a node at the *centroid* of each cell (see Fig. 1c) and the cell itself is treated as the CV. In this *Cell-Centred* approach,

* Tel.: +91 22 25767517; fax: +91 22 25726875.
E-mail address: awdate@me.iitb.ac.in

0017-9310/$ - see front matter © 2004 Elsevier Ltd. All rights reserved.
doi:10.1016/j.ijheatmasstransfer.2004.09.036

Nomenclature

AP, AE_k	coefficients in discretized equations
A_f	cell-face area
b_1^i	geometric coefficients
C	cell-face mass flow
d	diffusion coefficient
D	source term or diffusion coefficient
k	thermal conductivity
Nk	number of neighbouring cells of cell P
NVf	number of vertices forming a cell-face
NVT	number of vertices forming a cell
Pr	Prandtl number
p	pressure
R	residual
S	source term
t	time
u_i	Velocity in x_i-direction

Greek symbols

α	under-relaxation factor for velocity
β	under-relaxation factor for pressure or blending factor
β_1^i	geometric coefficients
μ	dynamic viscosity
ω	mass fraction
Δ	incremental value
ΔV	control volume
ρ	density
Φ	general variable
Γ	exchange coefficient
σ	normal stress
ξ_i	local curvilinear coordinates at the cell-face

Suffixes

B	refers to boundary node B
c	refers to face-centroid
f	refers to cell-face
k	refers to cell-face k
m	refers to mass conservation
n	refers to cell-face normal
P, E	refers to nodes P and E
sm	refers to smoothing
t	refers to turbulent
x_i	Refers to cartesian coordinates in i-direction

Superscripts

l	iteration counter
o	old Time
$-$	multidimensional average
$'$	correction

again the line joining neighbouring nodes, in general, will not intersect orthogonally with the cell-face shared by the neighbouring cells. In fact, in general, the point of intersection may lie on an extension of the cell-face rather than within it.

The above mentioned peculiarities of the unstructured meshes confound analysts having familiarity mainly with the structured (cartesian or curvilinear) grids. Further, on unstructured meshes, the nodes are identified serially through 1D arrays in an arbitrary manner and the familiar (i,j) in 2D and (i,j,k) in 3D identification is not available. This confounds understanding further.

In this paper, a discretization procedure within *cell-centred* approach is described by invoking a specially constructed *line-structure* so that those familiar with the structured-grid approaches can readily understand the main issues. Section 2 of the paper describes the transport equations involving a specially derived pressure-correction equation for colocated variables [5,8]. Section 3 describes the present discretization practice mentioned above for 3D cells. In this section, departures from practices of other researchers are mentioned. In Section 4, the overall calculation procedure is presented. Finally, conclusions are reported in Section 5. The dem-

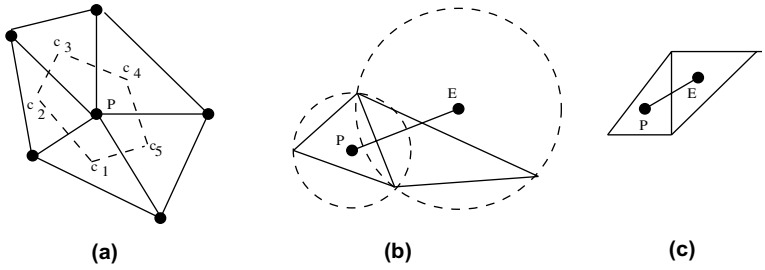

Fig. 1. Typical unstructured grids. (a) Vertex-centred, (b) circum-centred and (c) cell-centred.

onstration of validity of the present discretization practice is carried out in Part II [4].

2. Transport equations

Using tensor notation, the equations of mass, momentum and energy transfer can be written by a single equation for a general variable Φ. Thus,

$$\frac{\partial(\rho\Phi)}{\partial t}+\frac{\partial(q_j)}{\partial x_j}=\frac{\partial(\rho\Phi)}{\partial t}+\mathrm{div}(\vec{q})=S_\Phi \tag{1}$$

where $\vec{q}=(\vec{i}q_1+\vec{j}q_2+\vec{k}q_3)$ and

$$q_j=\rho u_j\Phi-\Gamma^{\Phi}_{\mathrm{eff}}\frac{\partial\Phi}{\partial x_j} \tag{2}$$

The meanings of Γ_{eff} and S_Φ for each Φ are listed in Table 1. Eq. (1) is called the *transport equation* for property Φ. In turbulent flows, the effective exchange coefficient Γ_{eff} is replaced by $\mu/Pr^{\Phi}+\mu_{\mathrm{t}}/Pr^{\phi}_{\mathrm{t}}$ for each Φ where suffix t denotes turbulent component. The turbulent viscosity μ_{t} is determined by solving additional scalar transport equations for variables characterizing turbulence. Typically, equations for turbulent kinetic energy e and its dissipation rate ϵ are solved [3] but, other variants are also possible. The additional scalar transport equations have the same form as Eq. (1).

When solutions to the above set of equations are sought, an algorithm for determining the pressure distribution must be devised. In the SIMPLE algorithm [1], the pressure is determined via a pressure-correction (p'_{m}) equation that satisfies the mass-conservation equation (that is, for $\Phi=1$). On unstructured meshes, it is most convenient to employ colocated variables so that scalar and vector variables are *defined* at the same location (or, node). For such a colocated (or, non-staggered) arrangement, Date [5,6,8] has derived an equation for *total* pressure-correction p' to eliminate the problem of zig-zagness in the predicted pressure. [1] For *compressible flows*, the equation has the following form

$$\frac{\partial'}{\partial x_i}\left[\Gamma^{p'}\frac{\partial p'}{\partial x_i}-\frac{U^*_i}{RT}p'\right]=\frac{\partial}{\partial x_i}\left[\rho\bar{u}_i-\frac{U^*_i}{RT}p'_{\mathrm{sm}}\right]+\frac{\partial\rho}{\partial t} \tag{3}$$

where

$$p'=p'_{\mathrm{m}}+p'_{\mathrm{sm}}=p'_{\mathrm{m}}+\frac{1}{2}(p-\bar{p}) \tag{4}$$

$$U^*_i=\bar{u}_i-\frac{\Gamma^{p'}}{\rho}\frac{\partial p'_{\mathrm{sm}}}{\partial x_i} \tag{5}$$

$$\Gamma^{p'}=\frac{\rho\alpha\Delta V}{AP^{u_i}} \tag{6}$$

[1] It may be noted that this method of removing zig-zagness in pressure prediction is different from that used by [13,9–11].

Table 1
Generalized representation of transport equations

Φ	$\Gamma^{\Phi}_{\mathrm{eff}}$	S_Φ
1	0	0
ω_k	$\rho(D+D_t)$	R_k
u_i	$\mu+\mu_t$	$-\partial p/\partial x_i+\rho B_i+S_{u_i}$
h	$(k+k_t)/C_{pm}$	Q'''
T	$(k+k_t)/C_{pm}$	Q'''/C_{pm}

In *incompressible* flows, $U^*_i=0$. The meanings of $\Gamma^{p'}$ and $\bar{u}_i$ will become clear in a later section. In Eq. (4), the evaluation of smoothing pressure-correction p'_{sm} requires evaluation of the space-averaged pressure $\bar{p}$. Sclichting [15] and Warsi [16] define this averaged pressure as one-third the negative sum of normal stresses (σ_{xi}). Date [8,5]. however, has shown that this average pressure can be expressed as

$$\bar{p}=-\frac{1}{3}(\sigma_{x1}+\sigma_{x2}+\sigma_{x3})=\frac{1}{3}(\bar{p}_{x1}+\bar{p}_{x2}+\bar{p}_{x3}) \tag{7}$$

where $\bar{p}_{xi}$ are independent solutions to $\partial^2 p/\partial x_i^2=0$.

3. Discretization

3.1. Gauss theorem

In the finite-volume formulation, Eq. (1) is first integrated over a cell-volume ΔV surrounding typical node P (see Fig. 2) so that

$$(\rho_P\Phi_P-\rho^{\mathrm{o}}_P\Phi^{\mathrm{o}}_P)\frac{\Delta V}{\Delta t}+\int_{\Delta V}\mathrm{div}\,\vec{q}\,\mathrm{d}V=S_\Phi\Delta V \tag{8}$$

The node P is defined at the centroid of the cell and its coordinates are given by

$$x_{i,P}=\frac{\sum_{n=1}^{\mathrm{NVT}}x_{i,n}}{\mathrm{NVT}} \tag{9}$$

where NVT are the number of vertices (4 for a tetrahedral cell and 8 for a hexahedral cell). The coordinates of vertices $x_{i,n}$ are known from the unstructured grid generator such as ANSYS. Now, to evaluate the volume integral in Eq. (8), Gauss's theorem is invoked. Thus,

$$\int_{\Delta V}\mathrm{div}\,\vec{q}\,\mathrm{d}V=\int_{A_{\mathrm{f}}}\vec{q}\cdot\vec{A}_{\mathrm{f}} \tag{10}$$

where $\int_{A_{\mathrm{f}}}$ is the surface integral and A_{f} is the surface area. The integral is now replaced by a summation.

$$\int_{A_{\mathrm{f}}}\vec{q}\cdot\vec{A}_{\mathrm{f}}=\sum_{k=1}^{Nk}(\vec{q}\cdot\vec{A}_{\mathrm{f}})k \tag{11}$$

where Nk represent the number of plane surfaces (or, the cell-faces) enclosing the cell-volume ΔV. For a tetrahedral cell, $Nk=4$ and for a hexahedral cell, $Nk=6$.

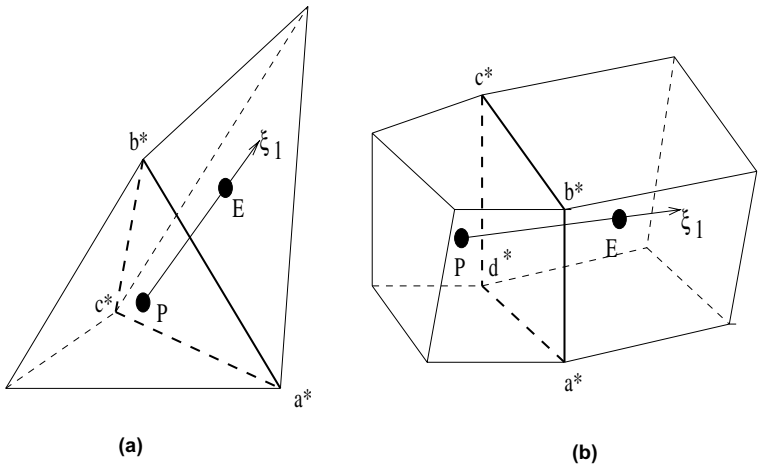

Fig. 2. Typical neighbouring cells P and E. (a) Tetrahedral cell and (b) hexahedral cell.

3.2. Cell-face area

To determine area of the kth cell-face, consider the triangular cell-face ($a^* - b^* - c^*$) of a tetrahedral cell shown in Fig. 2a. Then,

$$A_{f,k} = \sqrt{s(s - l_{a^*b^*})(s - l_{b^*c^*})(s - l_{a^*c^*})}$$
$$s = \frac{(l_{a^*b^*} + l_{b^*c^*} + l_{a^*c^*})}{2} \tag{12}$$

where lengths l can be determined from the known coordinates of the vertices. For hexahedral cells, the quadrilateral cell-face ($a^* - b^* - c^* - d^*$) is split into two triangles and Eq. (12) is again applied to determine the total area. This procedure can be applied to any polygonal cell-face by splitting the polygon into appropriate number of non-overlapping triangles.

3.3. Unit normal vector $\vec{n}$

The area vector is given by $\vec{A}_{fk} = A_{fk}\vec{n}$ where is $\vec{n}$ is the unit outward normal to the cell-face. To evaluate this vector, let the line joining neighbouring nodes P and E be in ξ_1 direction (see Fig. 3) and let ξ_2 and ξ_3 *coincide* with any two adjoining sides of the face-polygon. In Fig. 3, the two chosen sides merge at c^*. However, the choice of c^* is arbitrary. Now, the correct *directions* of ξ_2 and ξ_3 are determined such that coordinate system (ξ_1, ξ_2, ξ_3) obeys the right-hand-screw rule. This obedience is observed as shown below.

Let the unit normal vector be given by

$$\vec{n} = \vec{i}b_1^1 + \vec{i}b_1^2 + \vec{j}b_1^3 = \frac{\vec{k}\beta_1^1 + \vec{j}\beta_1^2 + \vec{k}\beta_1^3}{\sqrt{(\beta_1^1)^2 + (\beta_1^2)^2 + (\beta_1^3)^2}} \tag{13}$$

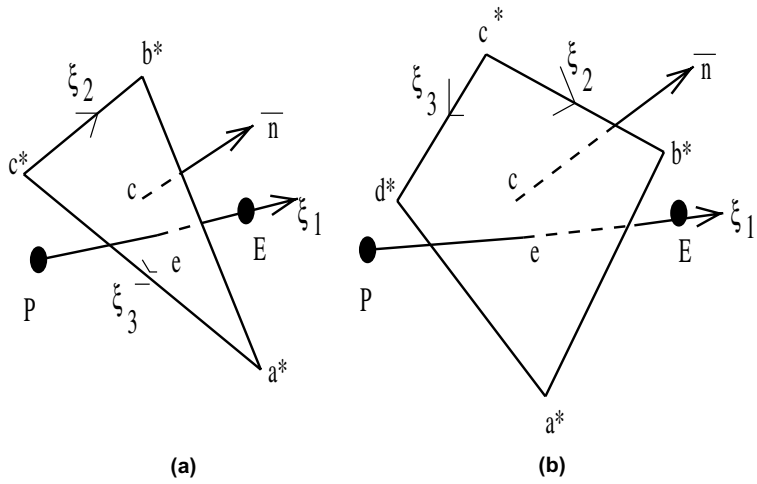

Fig. 3. Cell-face normal. (a) Tetrahedral cell and (b) hexahedral cell.

where

$$\beta_1^1 = \frac{\partial x_2}{\partial \xi_2}\frac{\partial x_3}{\partial \xi_3} - \frac{\partial x_3}{\partial \xi_2}\frac{\partial x_2}{\partial \xi_3}$$

$$\beta_1^2 = \frac{\partial x_3}{\partial \xi_2}\frac{\partial x_1}{\partial \xi_3} - \frac{\partial x_1}{\partial \xi_2}\frac{\partial x_3}{\partial \xi_3}$$

$$\beta_1^3 = \frac{\partial x_1}{\partial \xi_2}\frac{\partial x_2}{\partial \xi_3} - \frac{\partial x_2}{\partial \xi_2}\frac{\partial x_1}{\partial \xi_3} \tag{14}$$

Now, the correctness of directions ξ_2 and ξ_3 is ensured by requiring that the Jacobian J is *positive*. Thus,

$$J = \vec{a}_1 \cdot \vec{n} = \left(b_1^1 \frac{\partial x_1}{\partial \xi_1} + b_1^2 \frac{\partial x_2}{\partial \xi_1} + b_1^3 \frac{\partial x_3}{\partial \xi_1} \right) > 0 \tag{15}$$

where $\vec{a}_1$ is the base-vector tangent to coordinate line ξ_1. It is now a straightforward matter to determine coefficients of normal vector b_1^i and β_1^i once-for-all at every face of every cell.

3.4. Convective–diffusive transport

Making use of Eqs. (11)–(13), the total transport for the kth face can be written as

$$(\vec{q} \cdot \vec{A}_\mathrm{f})_k = (\vec{q} \cdot \vec{n})_k A_{\mathrm{f}k} = \sum_{i=1}^{3} (b_1^i q_i)_k A_{\mathrm{f}k} = q_{\mathrm{n}k} A_{\mathrm{f}k} \tag{16}$$

The normal flux $q_{\mathrm{n}k}$ is now assumed to be *uniform* over the cell-face area and explicitly evaluated at the *centroid* c of the cell-face (see Fig. 3). The coordinates of this centroid are

$$x_{ic} = \frac{\sum_{n=1}^{\mathrm{NVf}} x_{i,n}}{\mathrm{NVf}} \tag{17}$$

where NVf represents total number of vertices forming the kth cell-face. Thus, substituting Eq. (2) in Eq. (16), it can be shown that

$$\begin{aligned}(\vec{q} \cdot \vec{A}_\mathrm{f})_k &= (\vec{q} \cdot \vec{n})_{ck} A_{\mathrm{f}k} \\ &= \rho_{ck} A_{\mathrm{f}k} \Phi_{ck} \sum_{i=1}^{3} (b_1^i u_i)_{ck} \\ &\quad - \Gamma_{ck} A_{\mathrm{f}k} \sum_{i=1}^{3} \left[b_1^i \frac{\partial \Phi}{\partial x_i} \right]_{ck}\end{aligned} \tag{18}$$

For brevity, we now introduce following notations

$$C_{ck} = \rho_{ck} A_{\mathrm{f}k} \sum_{i=1}^{3} (b_1^i u_i)_{ck} \quad \text{face massflow} \tag{19}$$

$$\left.\frac{\partial \Phi}{\partial n}\right|_{ck} = \sum_{i=1}^{3} \left[b_1^i \frac{\partial \Phi}{\partial x_i} \right]_{ck} \quad \text{face} - \text{normal gradient} \tag{20}$$

where n is along the face-normal. Substituting Eqs. (19) and (20) in Eq. (18), therefore,

$$(\vec{q} \cdot \vec{A}_\mathrm{f})_k = C_{ck} \Phi_{ck} - \Gamma_{ck} A_{\mathrm{f}k} \left.\frac{\partial \Phi}{\partial n}\right|_{ck} \tag{21}$$

In the above expression, the first term on the right-hand side represents *convective* transport whereas the second term represents *diffusive* transport normal to the kth cell-face. The replacement indicated in Eq. (20) may be viewed as a special feature of the present discretization practice because the normal diffusion is sought to be evaluated directly rather than through its resolved components along x_i or ξ_i. Most previous researchers [9,11,10], it would appear, evaluate the normal diffusion through resolved components.

3.5. Construction of line-structure

Direct evaluation of face-normal transport requires *deliberate* construction of a *line-structure* at a cell-face. Existence of such a line-structure, however, is not obvious. The construction can be understood by considering triangular cell-face ($a^* b^* c^*$) of a tetrahedral cell-face shown in Fig. 4. In this figure, P and E are nodes straddling the cell-face. Line PE intersects the face at e. In general, e will not coincide with the face-centroid c. In fact, e may not even lie *within* the cell-face in general but may lie on an extension of the face-plane. However, this matter is inconsequential to further development.

The construction of the required line-structure begins by drawing two cell-face-normals through points c and e. Now, imagine a plane *parallel* to the cell-face passing through P. This plane will intersect the face-normal through c at P_2 and that through e at P_1. Triangle $P - P_1 - P_2$ will thus be parallel to the cell-face and the intersections at P_1 and P_2 will be orthogonal. Also, line P_1P_2 will be parallel to the line ce. A similar face-parallel plane passing through E will yield face-parallel triangle $E - E_1 - E_2$.

It is now obvious that the face-normal transport in Eq. (21) must be evaluated along line $P_2 - c - E_2$. This evaluation will now be analogous to that carried out at the cell-face of a structured grid.

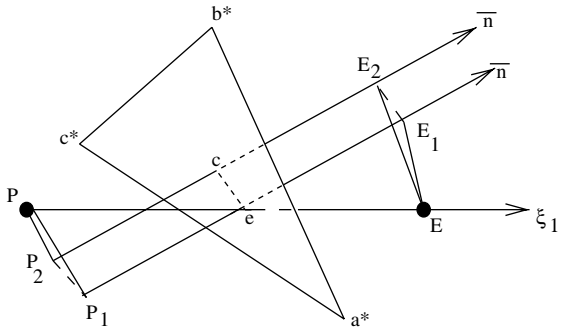

Fig. 4. Construction of a line-structure.

3.6. Discretized convection

Following the structured grid practice, the convective transport in Eq. (21) is evaluated as

$$C_{ck}\Phi_{ck} = C_{ck}[f_c\Phi_{P_2} + (1-f_c)\Phi_{E_2}]_k \tag{22}$$

where f_{ck} is a weighting factor that depends on the convection scheme used [2] and C_{ck} is evaluated from Eq. (19) as

$$C_{ck} = \rho_{ck}A_{fk}(b_1^1u_1 + b_1^2u_2 + b_1^3u_3)_{ck} \tag{23}$$

In the above evaluation, density and velocity components are evaluated by multidimensional averaging according to the following general formula

$$\Psi_{ck} = \frac{1}{2}[f_{mc}\Psi_{E_2} + (1-f_{mc})\Psi_{P_2}]_k + \frac{\Psi_{ck}}{2} \tag{24}$$

where

$$\overline{\psi}_{ck} = \frac{\sum_{n=1}^{NVf}\psi_n}{NVf} \tag{25}$$

and, from our construction,

$$f_{mc} = \frac{l_{P_2c}}{l_{P_2E_2}} = \frac{l_{P_1e}}{l_{P_1E_1}} = \frac{l_{Pe}}{l_{PE}} \tag{26}$$

where l_{Pe} and l_{PE} are evaluated from known coordinates of points P, e and E. In this paper, the weighting factor f_{ck} is evaluated by blending [11] of central-difference (CDS) and upwind-difference (UDS) schemes so that

$$f_{ck} = \beta(1-f_{mc}) + \frac{1}{2}(1-\beta)\left(1 + \frac{|\,C_{ck}\,|}{C_{ck}}\right) \tag{27}$$

where β is the blending factor, $\beta = 1$ corresponds to CDS whereas $\beta = 0$ corresponds to UDS.

In compressible flows, nearly discontinuous variations of Φ may occur in the presence of a shock. In such cases, it becomes important to sense the *shape* of the local Φ-profile via total variation diminishing (TVD) schemes. The convective-transport is then represented by [6]

$$\begin{aligned} C_{ck}\Phi_{ck} = {} & 0.5^*(C_{ck} + |\,C_{ck}\,|)(f^+\Phi_{E_2} + (1-f^+)\Phi_{W2}) \\ & + 0.5^*(C_{ck} - |\,C_{ck}\,|)(f^-\Phi_{P2} + (1-f^-)\Phi_{EE2}) \end{aligned} \tag{28}$$

where

$$f^+ = F\left[\frac{\Phi_{P2}-\Phi_{W2}}{\Phi_{E2}-\Phi_{W2}}\right] \quad f^- = F\left[\frac{\Phi_{E2}-\Phi_{EE2}}{\Phi_{P2}-\Phi_{EE2}}\right]$$

Points $W2$ and $EE2$, however, must be defined. With reference to our construction (see Fig. 4), the point $W2$ is defined to the *west* of $P2$ such that $l_{W2P2} = l_{P2c}$. Similarly, $EE2$ is defined to the *east* of $E2$ such that $l_{cE2} = l_{E2EE2}$. Both $W2$ and $EE2$ lie on the face-normal $P2$-c-$E2$. Finally, the profile-shape-sensing function $F[\,]$ can take variety of forms in different TVD schemes [14].

3.7. Discretized diffusion

For evaluating diffusion transport in Eq. (21), Γ_{ck} can be evaluated from Eq. (24) or, one may use harmonic mean of values at P_2 and E_2 [2]. Now, since point c may in general not be *midway* between points P_2 and E_2, using Taylor series expansion, the expression for second-order accurate face-normal gradient will read as

$$\begin{aligned} \left.\frac{\partial\Phi}{\partial n}\right|_c = {} & \frac{\Phi_{E_2}-\Phi_{P_2}}{l_{P_2E_2}} \\ & - \frac{(1-2f_{m,c})}{f_{m,c}(1-f_{m,c})}\left[\frac{f_{m,c}\Phi_{E_2} - \overline{\Phi}_c + (1-f_{m,c})\Phi_{P_2}}{l_{P_2E_2}}\right] \end{aligned} \tag{29}$$

where, from our construction,

$$l_{P_2E_2} = l_{P_1E_1} = \vec{l}_{PE}\cdot\vec{n} = \left|\sum_{i=1}^{3} b_1^i(x_{i,E} - x_{i,P})\right| \tag{30}$$

Therefore, the total diffusion transport in Eq. (21) can be expressed as

$$\begin{aligned} -\Gamma_{ck}A_{fk}\left.\frac{\partial\Phi}{\partial n}\right|_{ck} = {} & -d_{ck}(\Phi_{E_2}-\Phi_{P_2})_k \\ & + d_{ck}B_{ck}\left[f_{m,c}\Phi_{E_2} - \overline{\Phi}_c + (1-f_{m,c})\Phi_{P_2}\right]_k \end{aligned} \tag{31}$$

$$d_{ck} = \frac{\Gamma_{ck}A_{fk}}{l_{P_2E_2}} \tag{32}$$

and

$$B_{ck} = \frac{(1-2f_{m,c})}{f_{m,c}(1-f_{m,c})} \tag{33}$$

Note that d_{ck} is the familiar diffusion coefficient having significance of conductance. Symbol B_{ck} is introduced for brevity. Note that a Peclet number at the cell-face can be defined as $P_{ck} = C_{ck}/d_{ck}$. Thus, the weighting factor f_{ck} in Eq. (27) can also be sensitised to P_{ck} as required in hybrid or power-law schemes.

3.8. Interim discretization

Using above developments (Eqs. (21)–(33)), Eq. (8) can be written as

$$\begin{aligned} & (\rho_P\Phi_P - \rho_P^o\Phi_P^o)\frac{\Delta V}{\Delta t} + \sum_{k=1}^{Nk} C_{ck}[f_c\Phi_{P_2} + (1-f_c)\Phi_{E_2}]_k \\ & - \sum_{k=1}^{Nk} d_{ck}(\Phi_{E_2}-\Phi_{P_2})_k + \sum_{k=1}^{Nk} d_{ck}B_{ck}\left[f_{m,c}\Phi_{E_2} - \overline{\Phi}_c\right. \\ & \left. +(1-f_{m,c})\Phi_{P_2}\right]_k = S\Delta V \end{aligned} \tag{34}$$

In the above discretized equation, values of variables at fictitious points P_2 and E_2 and at vertices a^*, b^*, c^* are *not* known. These unknown values will now be expressed in terms of values at nodes P and E.

3.9. Interpolation of Φ at P_2, E_2, a^*, b^*, c^*

It is now assumed that variation of Φ in the neighbourhood of nodes P and E is multidimensionally linear. Then, Φ_{P_2}, for example, can be evaluated as

$$\Phi_{P_2} = \Phi_P + \Delta\Phi_P \tag{35}$$

where

$$\Delta\Phi_P = \vec{l}_{PP_2} \cdot \operatorname{grad}\Phi_P = \sum_{i=1}^{3}(x_{i,P_2} - x_{i,P})\left.\frac{\partial\Phi}{\partial x_i}\right|_P \tag{36}$$

Now, $(x_{i,P_2} - x_{i,P})$ is evaluated in terms of points whose coordinates are known. Thus, let

$$x_{i,P_2} - x_{i,P} = (x_{i,P_2} - x_{i,c}) + (x_{i,c} - x_{i,P}) \tag{37}$$

But, from our construction, $x_{i,P_2} - x_{i,c} = x_{i,P_1} - x_{i,e}$. Therefore, Eq. (37) is re-written as

$$x_{i,P_2} - x_{i,P} = (x_{i,P_1} - x_{i,e}) + (x_{i,e} - x_{i,P}) + (x_{i,c} - x_{i,e}) \tag{38}$$

But, the equation to the face-normal passing through e is given by

$$\vec{n} = \frac{\vec{i}(x_{1,e} - x_{1,P_1}) + \vec{j}(x_{2,e} - x_{2,P_1}) + \vec{k}(x_{3,e} - x_{3,P_1})}{l_{P_1e}} = \vec{i}b_1^1 + \vec{j}b_1^2 + \vec{k}b_1^3 \tag{39}$$

Therefore, it follows that

$$x_{i,P_1} - x_{i,e} = -l_{P_1e}b_1^i \tag{40}$$

Substituting the above equation in Eq. (38), therefore

$$x_{i,P_2} - x_{i,P} = lx_i + dx_i \tag{41}$$

where

$$\begin{aligned} lx_i &= x_{i,e} - x_{i,P} - l_{P_1e}b_1^i \\ dx_i &= x_{i,c} - x_{i,e} \end{aligned} \tag{42}$$

and

$$l_{P_1e} = \vec{l}_{Pe}.\vec{n} = \left|\sum_{i=1}^{3}(x_{i,e} - x_{i,P})b_1^i\right| \tag{43}$$

From the above developments, it follows that

$$\Phi_{P_2} = \Phi_P + \Delta\Phi_P = \Phi_P + \sum_{i=1}^{3}(lx_i + dx_i)\left.\frac{\partial\Phi}{\partial x_i}\right|_P \tag{44}$$

Invoking similar arguments, it can be shown that

$$\Phi_{E_2} = \Phi_E + \Delta\Phi_E = \Phi_E + \sum_{i=1}^{3}\left(dx_i - \frac{(1-f_{\mathrm{mc}})}{f_{\mathrm{mc}}}lx_i\right)\left.\frac{\partial\Phi}{\partial x_i}\right|_E \tag{45}$$

When TVD scheme is used, the values of Φ_{W2} and Φ_{EE2} are evaluated in analogous manner. Finally, value of Φ at each vertex of a cell-face is evaluated as average of two estimates. Thus, at vertex a^*, for example,

$$\Phi_{a^*} = \frac{1}{2}\left[\Phi_P + \vec{l}_{Pa^*} \cdot \operatorname{grad}\Phi_P + \Phi_E + \vec{l}_{Ea^*} \cdot \operatorname{grad}\Phi_E\right] \tag{46}$$

Similar estimates at other vertices enable calculation of $\overline{\Phi}_{\mathrm{c}}$.

3.10. Final discretization

Thus, using derivation of the previous sub-section, Eq. (34) can be written as

$$(\rho_P\Phi_P - \rho_P^{\mathrm{o}}\Phi_P^{\mathrm{o}})\frac{\Delta V}{\Delta t} + \sum_{k=1}^{Nk} C_{\mathrm{c}k}[f_{\mathrm{c}}\Phi_P + (1-f_{\mathrm{c}})\Phi_E]_k - \sum_{k=1}^{Nk} d_{\mathrm{c}k}(\Phi_E - \Phi_P)_k = S\,\Delta V + \sum_{k=1}^{Nk} D_k \tag{47}$$

where

$$D_k = -d_{\mathrm{c}k}b_{\mathrm{c}k}[f_{mc}(\Phi_E + \Delta\Phi_E) - \overline{\Phi}_{\mathrm{c}} + (1-f_{mc}) \times (\Phi_P + \Delta\Phi_P)]_k + d_{\mathrm{c}k}(\Delta\Phi_E - \Delta\Phi_P)_k - C_{\mathrm{c}k}[f_{\mathrm{c}}\Delta\Phi_P + (1-f_{\mathrm{c}})\Delta\Phi_E]_k \tag{48}$$

3.10.1. Further simplification

Grouping terms in Φ_P, Eq. (47) is now re-written as

$$AP\Phi_P = \sum_{k=1}^{Nk} AE_k\Phi_{E,k} + S\,\Delta V + \frac{\rho_{\mathrm{m},P}^{\mathrm{o}}\Delta V}{\Delta t}\Phi_P^{\mathrm{o}} + \sum_{k=1}^{Nk} D_k \tag{49}$$

where

$$AE_k = d_{\mathrm{c}k} - (1-f_{\mathrm{c}k})C_{\mathrm{c}k} \tag{50}$$

$$AP = \frac{\rho_P\Delta V}{\Delta t} + \sum_{i=1}^{3}[C_{\mathrm{c}k}f_{\mathrm{c}k} + d_{\mathrm{c}k}] \tag{51}$$

Now, for $\Phi = 1$ (that is, mass conservation), Eq. (34) gives

$$(\rho_P - \rho_P^{\mathrm{o}})\frac{\Delta V}{\Delta t} + \sum_{k=1}^{Nk} C_{\mathrm{c}k} = 0 \tag{52}$$

Replacing $\rho_P\Delta V/\Delta t$ in Eq. (51) via the above equation, it follows that

$$AP = \rho_P^{\mathrm{o}}\frac{\Delta V}{\Delta t} + \sum_{k=1}^{Nk} AE_k \tag{53}$$

With the above expression for AP, Eq. (49) suitable for computer implementation in an iterative procedure reads as

$$AP\Phi_P^{l+1} = \sum_{k=1}^{Nk} AE_k\Phi_{E,k}^{l+1} + S^l\,\Delta V + \frac{\rho_P^{\mathrm{o}}\Delta V}{\Delta t}\Phi_P^{\mathrm{o}} + \sum_{k=1}^{Nk} D_k^l \tag{54}$$

where superscript l denotes iteration counter. The equation shows that S and D_k terms lag behind Φ values by one iteration. Eq. (54) is the main discretized transport equation for node P. The equation is valid for cells of any topology as well as any polygonal plane cell-face.

3.11. Evaluation of cartesian gradients

The evaluation of D_k terms requires evaluations of $\Delta\Phi_P$ and $\Delta\Phi_E$ (see Eq. (48)). The latter terms, in turn, require evaluations of cartesian gradients (see Eqs. (44) and (45)) at nodal positions P. This evaluation is carried out as follows

$$\left.\frac{\partial\Phi}{\partial x_i}\right|_P = \left.\frac{\overline{\partial\Phi}}{\partial x_i}\right|_P = \frac{1}{\Delta V}\int_{\Delta V}\left.\frac{\partial\Phi}{\partial x_i}\right|_P \mathrm{d}V = \frac{1}{\Delta V}\int_{A_\mathrm{f}}(b_1^i\Phi)dA_\mathrm{f} = \frac{1}{\Delta V}\sum_{k=1}^{Nk}(b_1^i\Phi)_{\mathrm{c}k}A_{\mathrm{f}k} \tag{55}$$

where $\Phi_{\mathrm{c}k}$ is evaluated from Eq. (24) which again requires $\Delta\Phi_P$ and $\Delta\Phi_E$ to complete evaluations of Φ_{P_2} and Φ_{E_2} This makes Eq. (55) implicit in $\partial\Phi/\partial x_i|_P$. However, since the overall procedure is iterative, such implicitness is acceptable.

3.12. Boundary conditions

Consider a cell near a domain boundary (Fig. 5) with the cell-face coinciding with the boundary. A boundary node B is now *defined* at the centroid of the cell-face (a^*, b^*, c^*) so that with our usual notation $B = c = e$ and coordinates of B can be readily evaluated from those of face-vertices. [2] Now, let P_2B be the outward normal to the boundary face and PP_2 be orthogonal to P_2B and, therefore, parallel to the boundary face. Then, the total outward transport through the boundary face is given by

$$(\vec{q}\cdot\vec{A}_\mathrm{f})_\mathrm{B} = C_\mathrm{B}\Phi_\mathrm{B} - (\Gamma A_\mathrm{f})_\mathrm{B}\left.\frac{\partial\Phi}{\partial n}\right|_\mathrm{B} \tag{56}$$

where

$$C_\mathrm{B} = \rho_\mathrm{B}A_{\mathrm{f},\mathrm{B}}\sum_{i=1}^{3}b_1^i u_{i,\mathrm{B}} \tag{57}$$

$$C_\mathrm{B}\Phi_\mathrm{B} = C_\mathrm{B}[f_\mathrm{B}\Phi_{P_2} + (1-f_\mathrm{B})\Phi_\mathrm{B}] \tag{58}$$

$$\left.\frac{\partial\Phi}{\partial n}\right|_\mathrm{B} = \frac{(\Phi_\mathrm{B}-\Phi_{P_2})}{l_{P_2B}} = \frac{(\Phi_\mathrm{B}-\Phi_P-\Delta\Phi_P)}{l_{P_2B}} \tag{59}$$

[2] Note that points B, c and e will now coincide. Similarly points P_2 and P_1 will also coincide for the boundary face.

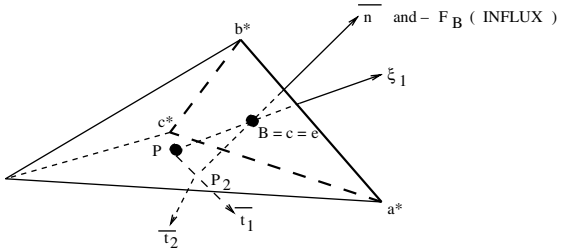

Fig. 5. Typical near-boundary cell.

Therefore, Eq. (56) can be written as

$$(\vec{q}\cdot\vec{A}_\mathrm{f}) = C_\mathrm{B}[f_\mathrm{B}(\Phi_P+\Delta\Phi_P) + (1-f_\mathrm{B})\Phi_\mathrm{B}] - d_\mathrm{B}[\Phi_\mathrm{B}-\Phi_P-\Delta\Phi_P] \tag{60}$$

where $d_\mathrm{B} = \Gamma_\mathrm{B}A_{\mathrm{f}\mathrm{B}}/l_{P_2\mathrm{B}}$.

3.12.1. Scalar variables

For the near-boundary cell, Eq. (54) is written as

$$AP\Phi_P^{l+1} = \sum\nolimits_{k=1}^{Nk-B}AE_k\Phi_{E,k}^{l+1} + S^l\Delta V + \frac{\rho_{\mathrm{m},P}^\mathrm{o}\Delta V}{\Delta t}\Phi_P^\mathrm{o} + \sum_{k=1}^{Nk-B}D_k^l - (\vec{q}\cdot\vec{A}_\mathrm{f})_\mathrm{B} \tag{61}$$

where *Nk-B* implies that boundary-face contribution is *excluded* from the summation (the same applies to the AP coefficient, Eq. (53)) and accounted through—$(\vec{q}\cdot\vec{A}_\mathrm{f})_\mathrm{B}$ term. For a scalar variable, Φ_B or *influx* $F_\mathrm{B} = \Gamma_\mathrm{B}\partial\Phi/\partial n|_\mathrm{B}$ are typically specified. In either case, employing Eq. (60) and *source-term linearization* practice [2], Eq. (61) can be appropriately modified.

3.12.2. Vector variables

At *inflow* and *wall* boundaries, the velocities $U_{i,\mathrm{B}}$ are known and, therefore, Eq. (61) readily applies. Care, however, is needed when *exit* and *symmetry* boundaries are specified. Thus,

At symmetry boundary

$$U_{n,\mathrm{B}} = 0 \quad \text{and} \quad \partial U_t/\partial n|_\mathrm{B} = 0$$

At exit boundary

$$\partial U_n/\partial n|_\mathrm{B} = 0 \quad \text{and} \quad \partial U_t/\partial n|_\mathrm{B} = 0$$

where U_n and U_t are face-normal and face-tangent velocities. Thus,

$$U_n = \vec{V}\cdot\vec{n} = \sum_{i=1}^{3}b_1^i u_i \tag{62}$$

Now, to evaluate the face-tangent velocities, we construct an orthogonal coordinate system $(\vec{n},\vec{t}_1,\vec{t}_2)$ where $\vec{t}_1$ and $\vec{t}_2$ are two tangent vectors parallel to the boundary-face. One of these (say, $\vec{t}_1$) can be taken along line PP_2. The second one $\vec{t}_2$ will now be orthogonal to $\vec{t}_1$ and $\vec{n}$. Thus, from Eq. (41) (with $dx_i = 0$ because B, c and e coincide)

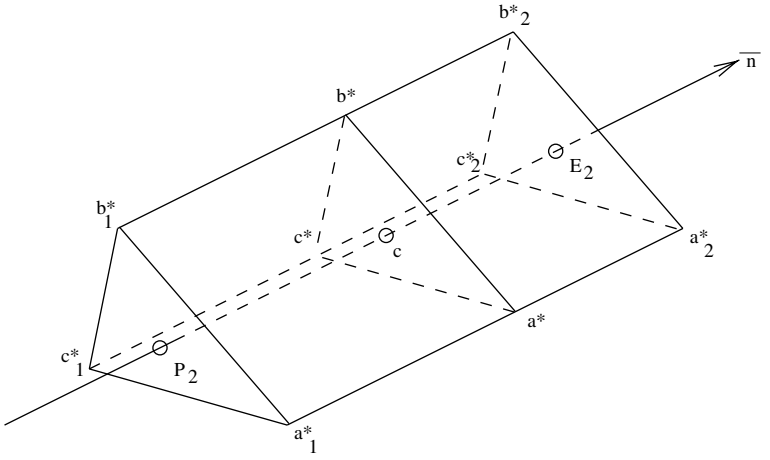

Fig. 6. Control volume at the cell-face.

$$\vec{t}_1 = \vec{i}lx_1 + \vec{j}lx_2 + \vec{k}lx_3 \tag{63}$$

and

$$\vec{t}_2 = \vec{n} \times \vec{t}_1 = \vec{i}mx_1 + \vec{j}mx_2 + \vec{k}mx_3 \tag{64}$$

where $mx_1 = b_1^2 lx_3 - b_1^3 lx_2$, $mx_2 = b_1^3 lx_1 - b_1^1 lx_3$, $mx_3 = b_1^1 lx_2 - b_1^2 x_1$. It is now a straight forward matter to implement the *symmetry* boundary condition, for example, via the following three equations.

Symmetry boundary

$$U_{n,\mathrm{B}} = \sum_{i=1}^{3} b_1^i u_{i,\mathrm{B}} = 0 \tag{65}$$

$$\left.\frac{\partial U_{t_1}}{\partial n}\right|_{\mathrm{B}} = 0 \quad U_{t_1,\mathrm{B}} = U_{t_1,P_2}$$
$$\sum_{i=1}^{3} lx_i u_{i,\mathrm{B}} = \sum_{i=1}^{3} lx_i u_{i,P_2} = \sum_{i=1}^{3} lx_1 (u_{i,P} + \Delta u_{i,P}) \tag{66}$$

$$\left.\frac{\partial U_{t_2}}{\partial n}\right|_{\mathrm{B}} = 0 \quad U_{t_1,\mathrm{B}} = U_{t_1,P_2}$$
$$\sum_{i=1}^{3} mx_i u_{i,\mathrm{B}} = \sum_{i=1}^{3} mx_i u_{i,P_2} = \sum_{i=1}^{3} mx_i (u_{i,P} + \Delta u_{i,P}) \tag{67}$$

The above three equations can be solved simultaneously to obtain three boundary velocities $u_{i,\mathrm{B}}$. Similarly, to implement the *exit* boundary condition, only Eq. (65) needs to be modified to read as

Exit boundary

$$\left.\frac{\partial U_n}{\partial n}\right|_{\mathrm{B}} = 0 \quad U_{n,\mathrm{B}} = U_{n,P_2}$$
$$\sum_{i=1}^{3} b_1^i u_{i,\mathrm{B}} = \sum_{i=1}^{3} b_1^i u_{i,P_2} = \sum_{i=1}^{3} b_1^i (u_{i,P} + \Delta u_{i,P}) \tag{68}$$

3.13. Pressure-correction equation

For simplicity, a discretized version of the incompressible form ($U_i^* = 0$) of the pressure-correction Eq. (3) is given below.

$$AP p'_P = \sum_{k=1}^{Nk} AE_k p'_{E,k} - \sum_{i=1}^{Nk} C_{\mathrm{c}k}^{l} - (\rho_P - \rho_P^{\mathrm{o}}) \frac{\Delta V}{\Delta t} + \sum_{k=1}^{Nk-B} D_k^{p'} \tag{69}$$

where $AP = \sum_{k=1}^{Nk} AE_k$ and, from Eq. (6)

$$AE_k = \frac{\Gamma_{ck}^{p'} A_{\mathrm{f}k}}{l_{P_2E_2}} = \left[\frac{\rho_{\mathrm{m}}^{l} \alpha \Delta V}{AP^{u_i}}\right]_{ck} \frac{A_{\mathrm{f}k}}{l_{P_2E_2}} \tag{70}$$

The $D_k^{p'}$ term contains gradients of p'. However, during iterative process in SIMPLE, the pressure-correction equation is treated only as an estimator of p'. Hence, $D_k^{p'}$ may be set to zero. Further, evaluation of AE_k requires evaluations of $AP_{ck}^{u_i}$ and ΔV_{ck}. The former is evaluated by harmonic mean [5] but the evaluation of the latter requires construction of another line-structure at the cell-face. This construction is shown in Fig. 6 for a triangular cell-face of a tetrahedral cell.

The construction involves drawing triangles (a^*_1, b^*_1, c^*_1) at P_2 and (a^*_2, b^*_2, c^*_2) at E_2 such that the planes of these triangles are parallel to the parent cell-face (a^*, b^*, c^*). Joining vertices of these triangles completes construction of cell-face control-volume ΔV_{ck}. Thus, [3]

[3] Note that, in general, if the parent, cell-face were n-polygon, ΔV_{ck} will be an n-polygonal cylinder having $(n + 2)$ faces.

$$\Delta V_{ck} = A_{fk} l_{P_2E_2} \tag{71}$$

and, from Eq. (70),

$$AE_k = \frac{\rho^l_{m,ck} \alpha A^2_{fk}}{AP^{u_i}_{ck}} \tag{72}$$

Eq. (69) is solved with boundary condition $\partial p'/\partial n|_B = 0$. If the boundary pressure is specified then $p'_B = 0$. After solving Eq. (69), the mass-conserving pressure-correction distribution is recovered from Eq. (4) [5,6,8]. This, however, requires evaluation of *smoothing pressure-correction* p'_{sm} and, hence, of $\bar{p}^l$.

Evaluation of $\bar{p}^l$

As shown in Eq. (7), we need to evaluate $\bar{p}^l{}_{xi}$ as solutions $\partial^2 p/\partial x_i^2|_P$. Thus,

$$\frac{1}{\Delta V}\int_{\Delta V} \left.\frac{\partial^2 p}{\partial x_i^2}\right|_P \mathrm{d}V = \frac{1}{\Delta V}\sum_{k=1}^{Nk} \left[b^i_1 A_f\right]_k \left.\frac{\partial p^l}{\partial x_i}\right|_{ck} = 0 \tag{73}$$

Now, to evaluate the cell-face pressure-gradient $\partial p^1/\partial x_i|_{ck}$, Gauss-theorem is applied to ΔV_{ck}. The resulting algebra is somewhat lengthy and, therefore, only the final result for *triangular cell-face* is given below.

$$\bar{p}_{xl,P} = \frac{\sum_{k=1}^{Nk}(A_{1l} - A_{2l} + A_{3l})}{\sum_{k=1}^{Nk} A_{4l}} \quad l,m,n \quad \text{cyclic} \tag{74}$$

where

$$A_{1l} = \frac{(b^l_1 A_{fk})^2}{\Delta V_{ck}}(p_E + \Delta p_E - \Delta p_P)_k \tag{75}$$

$$A_{2l} = \frac{b^l_1 b^m_1}{2}[p_{a^*}(x_{n,c^*} - x_{n,b^*}) + p_{b^*}(x_{n,a^*} - x_{n,c^*}) + p_{c^*}(x_{n,b^*} - x_{n,a^*})] \tag{76}$$

$$A_{3l} = \frac{b^l_1 b^n_1}{2}[p_{a^*}(x_{m,c^*} - x_{m,b^*}) + p_{b^*}(x_{m,a^*} - x_{m,c^*}) + p_{c^*}(x_{m,b^*} - x_{m,a^*})] \tag{77}$$

$$A_{4l} = \frac{(b^l_1 A_{fk})^2}{\Delta V_{ck}} \tag{78}$$

where, the pressures at the cell-face vertices are evaluated in the manner of Eq. (46).

4. Overall calculation procedure

The overall SIMPLE procedure for colocated grids is as follows:

Preliminaries

1. For the domain of interest, generate unstructured mesh using mesh-generator such as ANSYS. The mesh generator provides two files:
   (a) Vertex file in which all vertices are serially numbered along with the coordinates x_i of each vertex.
   (b) Element file in which elements (or nodes) are serially numbered along with the number identifications of vertices forming the element.
2. Using the information in the above two files, identify neighbouring nodes of each node N. This identification is easily carried out because the neighbouring nodes must share the same cell-face and hence, the same vertex numbers. If no shared cell-face is identified then the cell-face must be the boundary face. Hence, define a boundary node and assign a node number to it. For each node N, store the node number of neighbouring node in an array NABOR (N,K) where K is the kth cell-face.
3. Now, carry out identification of ξ_2 and ξ_3 directions as indicated in Section 3.3 at each cell-face of every cell.
4. With the above information at hand, it is now easy to evaluate b^i_1, lx_i, dx_i, fmc_k and A_{fk} once-for-all. Also, evaluate cell-volume.

Solution Begins

5. At a given time step, guess pressure field p^l.
6. Solve once Eq. (54) for $\Phi = u_i$ to yield u^l_i distribution. The solution is preceded by evaluation of coefficients AE_k and by accounting for boundary' conditions.
7. Perform maximum 10 iterations of p' Eq. (69) where AE_k are evaluated from Eq. (72).
8. Recover *mass-conserving* pressure-correction p'_m according to Eq. (4) by evaluating p'_{sm}. The latter requires evaluation of $\overline{p^l}$. This average pressure is evaluated from Eq. (7) where $\overline{p^l}_{xi}$ are evaluated using Eq. (74). This step ensures that the predicted pressures do not exhibit zig-zag behaviour [8].
9. Apply pressure and velocity corrections at each node. Thus

$$p^{l+1}_P = p^l_P + \beta p'_{m,P} \quad 0 < \beta < 1 \tag{79}$$

$$u^{l+1}_{i,P} = u^l_{i,P} - \frac{\alpha \Delta V}{AP^{u_i}} \left.\frac{\partial p'_m}{\partial x_i}\right|_P \tag{80}$$

where α is the under-relaxation factor used in momentum equations.

10. Solve Eq. (54) for all other relevant scalar Φ's.
11. Evaluate residuals from imbalance in Eq. (54) for all Φ's according to

$$R_\Phi = \left[\sum_{\text{all nodes}} \left\{AP\Phi_P - \sum_k AE_k \Phi_{Ek} - S^\Phi_{\text{total}}\right\}^2\right]^{0.5} \tag{81}$$

The mass residual is evaluated as

$$R_m = \left[\sum_{\text{all nodes}} \left\{ AP p'_{\mathrm{m},P} - \sum_k AE_k p'_{\mathrm{m},Ek} \right\}^2 \right]^{0.5} \quad (82)$$

where the coefficients AP and AE_k are taken from (69). This practice for evaluation of R_{m} is special to the present procedure. The reasons are explained in [5,8].

12. If convergence criterion is not satisfied, treat $p^{l+1} = p^l$ and $\Phi^{l+1} = \Phi^l$ and return to step 6.
13. To execute the next time step, set all $\Phi^{\mathrm{o}} = \Phi^{l+1}$ and return to step 5.

5. Conclusions

(1) In this paper, procedure for discretization of three-dimensional transport equations on unstructured meshes is described. The procedure is applicable to cells of any topology provided the cell-faces are plane surfaces.

(2) The discretization is carried out by constructing a special *line structure* so that evaluations at the cell-faces can be carried out in structured-grid-like manner.

(3) The paper presents implementation aspects of *smoothing* pressure-correction on unstructured meshes using cell-centered discretization.

References

[1] S.V. Patankar, D.B. Spalding, A calculation procedure for heat mass and momentum transfer in three dimensional parabolic flows, Int. J. Heat Mass Transfer 15 (1972) 1787–1806.
[2] S.V. Patankar, Numerical Heat Transfer and Fluid Flow, Hemisphere Publishing Corp., New York, 1980.
[3] B.E. Launder, D.B. Spalding, Mathematical Models of Turbulence, Academic Press, New York, 1972.
[4] A.W. Date, Solution of transport equations on unstructured meshes with cell-centered colocated variables. Part II. Applications, Companion Paper.
[5] A.W. Date, Complete pressure correction algorithm for solution of incompressible Navier–Stokes equations on a non-staggered grid, Numer. Heat Transfer, Part B 29 (1995) 441–458.
[6] A.W. Date, Solution of Navier–Stokes equations on non-staggered grids at all speeds, Numer. Heat Transfer, Part B 33 (1998) 451–467.
[7] A.W. Date, Smoothing pressure correction on unstructured Mesh, in: Proc. 2nd ICHMT Conference on Advances in Computational Heat Transfer, Palm Cove, Australia, May 2001.
[8] A.W. Date, Fluid dynamical view of pressure checkerboarding problem and smoothing pressure correction on meshes with colocated variables, Int. J. Heat Mass Transfer 46 (2003) 4885–4898.
[9] L. Davidson, A pressure correction method for unstructured meshes with arbitrary control volumes, Int. J. Numer. Meth. Fluids 22 (1996) 265–281.
[10] S.R. Mathur, J.Y. Murthy, A pressure-based method for unstructured meshes, Numer. Heat Transfer, Part B 31 (1997) 195–215.
[11] I. Demirdzic, S. Muzaferija, Numerical method for coupled fluid flow, heat transfer and stress analysis using unstructured moving meshes with cells of arbitrary topology, Comput. Meth. Appl. Mech. Eng. 125 (1995) 235–255.
[12] H. Choi, D. Lee, J.S. Maeng, A node-centred pressure-based method for all speeds on unstructured meshes, Numer. Heat Transfer, Part B 44 (2003) 165–185.
[13] C. Prakash, S.V. Patankar, A control volume-based finite element method for solving Navier–Stokes equations using equal-order velocity–pressure interpolation, Numer. Heat Transfer 8 (1985) 259–280.
[14] C.H. Lin, C.A. Lin, Simple high-order bounded convection scheme to model discontinuities, AIAA J. (35) (1997) 563–565.
[15] H. Schlichting, Boundary-Layer Theory English translation by J. Kestin, sixth ed., McGraw-Hill, 1968.
[16] Z.U.A. Warsi, Fluid Dynamics—Theoretical and Computational Approaches, CRC Press, London, 1993.